THE ANATOLIAN JOURNAL OF CARDIOLOGY

Official journal of the TURKISH SOCIETY OF CARDIOLOGY

Identification of Biomarkers for Acute Myocardial Infarction Based on Cell Senescence Genes and Machine Learning

ABSTRACT

Background: This study aims to identify senescence-related biomarkers for ST-elevation myocardial infarction (STEMI) prognosis.

Methods: RNA expression data for STEMI samples and controls were obtained from the gene expression omnibus (GEO) database, and cellular senescence genes were acquired from CellAge database. Differential and overlap analyses were used to identify differentially expressed cellular senescence-related genes (DE-SRGs) in STEMI samples. Differentially expressed cellular senescence-related genes were further analyzed by plotting receiver operating characteristic (ROC) curves and machine learning algorithms. Gene Set Enrichment Analysis (GSEA) was employed on each biomarker. Immune-related analyses, competing endogenous RNA (ceRNA) construction, and target drug prediction were performed on biomarkers.

Results: This study identified 7 DE-SRGs for STEMI prognosis. Gene Set Enrichment Analysis results showed enriched pathways, including ribosomes, autophagy, allograft rejection, and autoimmune thyroid disease. Furthermore, T cells, CD4 memory resting T cells, gamma delta, monocytes, and neutrophils represented signifi antly different proportions between STEMI samples and controls. In addition, CEBPB was positively correlated with monocytes and neutrophils but negatively correlated with T-cell CD8. A ceRNA network was established, and 8 FDA-approved drugs were predicted.

Conclusion: This study identified 7 cellular senescence-related biomarkers, which could lay a foundation for further study of the relationship between STEMI and cellular senescence.

Keywords: ST-elevation myocardial infarction, cellular senescence, biomarkers, gene set enrichment analysis, immune infilt ation

ORIGINAL INVESTIGATION

INTRODUCTION

ST-segment elevation myocardial infarction (STEMI) is characterized by an acute reduction in myocardial blood fl w and is triggered by a complete obstruction of the coronary artery at the location of a preexisting atherosclerotic plaque, plaque erosion, or calcific nodules.[1,2] Over 2 million people worldwide are diagnosed with STEMI each year, which has caused STEMI to become a major cause of morbidity and mortality.[3] Symptoms of STEMI often present as heavy or pressured chest pain, shortness of breath, sweating, nausea or vomiting, feeling lightheaded or dizzy, and fatigue.[4] The diagnosis of STEMI is based on history, characteristic symptoms, and electrocardiogram changes. In addition, an echocardiogram can be useful for ruling out acute STEMI. Moreover, the biomarkers troponin I or T are of high clinical sensitivity and specificity for myocardial tissues.[5] However, the guidelines recommend immediate reperfusion therapy without waiting for biomarker results for STEMI patients (with symptoms of ischemia for ≤12 hours and persistent ST-segment elevation).[6] The treatment of STEMI includes reperfusion therapy, thrombolytic therapy, medical management, and cardiac rehabilitation.[2,5] Although various methods are available, STEMI patients are still limited in their treatment options because of narrow treatment windows and delays in recognition and treatment.

Liya Li[1,2]
Pei Qin[1]

[1]*Department of Anesthesiology, Xi'an Children's Hospital, Xi'an, China*
[2]*Department of Anesthesiology, The Second Affilia ed Hospital of Dalian Medical University, Dalian, China*

Corresponding author:
Pei Qin
✉ xiaoqinnuli2011@126.com

Received: January 9, 2025
Accepted: April 15, 2025
Available Online Date: July 9, 2025

Cite this article as: Li L, Qin P. Identification of biomarkers for acute myocardial infarction based on cell senescence genes and machine learning. *Anatol J Cardiol.* 2025;29(8):409-422.

DOI:10.14744/AnatolJCardiol.2025.5129

Cellular senescence is a natural process that leads to irreversible growth arrest and contributes to tissue aging and homeostasis.[7] However, it is also increasingly recognized as a key driver of various diseases, including cancer, cardiovascular disease, neurodegenerative disorders, and metabolic disorders.[8] The accumulation of senescent cells in tissues can trigger chronic inflammation, alter tissue architecture, impair tissue regeneration and repair, and promote the development and progression of various diseases. As such, targeting senescent cells has emerged as a promising therapeutic approach for age-related diseases. Senescent cells are detrimental to all stages of atherosclerosis. These cells can promote infla - mation, oxidative stress, and matrix degradation, leading to plaque rupture and thrombosis.[9] Additionally, senescent cells in the myocardium can impair cardiac function and tissue repair, exacerbating the damage caused by STEMI.[10] Hence, inhibition of senescence may be a potential therapeutic strategy for STEMI, as it prevents or attenuates the deleterious effects of senescent cells and promotes tissue healing and regeneration.[11] Overall, senescence of different cardiac cells is one of the causes of pathophysiological changes such as atherosclerosis, myocardial infarction, and cardiac fib osis, including STEMI.[10] More research is needed to fully elucidate these mechanisms and identify new therapeutic strategies for preventing or treating STEMI. Therefore, this study aimed to identify biomarkers associated with cellular senescence in STEMI and explore potential therapeutic agents.

METHODS

Data Collection

GSE60993 and GSE62646 datasets were downloaded from gene expression omnibus (GEO) database (https://www.ncbi.nlm.nih.gov/geo/). GSE60993 comprises the transcriptome data of peripheral blood from acute coronary syndrome (ACS) patients, which had 17 disease samples (7 STEMI), 10 non-ST-elevation MI (NSTEMI), and 7 normal controls. GSE62646 includes the expression profile of blood samples from 28 STEMI patients and 14 stable coronary artery disease patients without a history of myocardial infarction. Additionally, according to Avelar et al,[12] 279 human genes driving cellular senescence were acquired from CellAge database (http://genomics.senescence.info/cells). Finally, an immunomodulator list was downloaded from TISIDB database (http://cis.hku.hk/TISIDB/index.php) based on the research of Xu et al.[13]

HIGHLIGHTS

- The work has proposed identifying ST-elevation myocardial infarction based on DE-SRGs segmentation.
- Cell aging triggers inflammation, tissue regeneration, and repair, contributing to STEMI.
- Identifying cell aging biomarkers in STEMI based on GSEA, ROC curves, and machine-learning algorithms.
- Target long non-coding RNAs (lncRNAs) were predicted by the ceRNA network.
- Computational tools were used for drug prediction and molecular docking.

Identifi ation and Functional Enrichment Analyses of DE-SRGs

Limma package (version 3.48.3)[14] was initially applied to distinguish differentially expressed genes (DEGs) between 17 STEMI samples and 7 controls from GSE60993. Genes satisfied $P < .05$ and $|logFC|>0.5$ were selected as DEGs, which would be presented in a volcano map by ggplot2 (version 3.3.5) and a heat map by pheatmap (version 1.0.12) (https://rdocumentation.org/packages/pheatmap/versions/1.0.12), and further overlapped with the 279 cellular senescence-related genes (SRGs), and the intersected genes were regarded as differentially expressed cellular senescence-related genes (DE-SRGs). Subsequently, gene ontology (GO) and Kyoto Encyclopedia of Genes and Genomes (KEGG) pathway enrichment analyses were employed on DE-SRGs by clusterProfiler (version 4.0.5)[15] with the threshold set as $P < .05$.

Screening of Biomarkers

For preliminary screening DE-SRGs with diagnostic values, ROC curves of them were fir tly drawn, and the DE-SRGs with AUCs greater than 0.85 were considered as DE-SRGs with diagnostic value. Then, DE-SRGs with diagnostic values were further analyzed through 3 machine learning algorithms (generalized linear model (GLM), random forest (RF), and support vector machine (SVM)). Generalized Linear Model is a traditional statistical model commonly used in regression analysis.[16] Random Forest is a machine learning algorithm used for classifi ation and regression problems, which makes predictions by aggregating multiple decision trees. Random Forest builds a predictive model by sampling both objects and variables, generating multiple decision trees, and classifying objects sequentially.[17] The classifi ation results from each decision tree are then aggregated, and the majority class among all predicted categories is considered the predicted class for the object, which improves classifi ation accuracy. Compared to other classifi ation methods, RF typically offers the following advantages: higher classifi ation accuracy; the ability to effectively handle high-dimensional (multivariate) datasets without the need for dimensionality reduction; advantages in processing large datasets; applicability to datasets with many missing values; and the ability to measure the relative importance of variables during classifi ation. For the RF model, we seted ntree = 1000: This was the number of trees in the model. It specified that 1000 trees should be built; nPerm = 50: Used to evaluate feature importance, it referred to the number of times each feature was perturbed when calculating feature importance, seted to 50 here; mtry = floor(sqrt(n ol(RFdata) – 1)): Defined the number of features to be randomly selected for each tree during construction; proximity = T: This indicated that the proximity (similarity) between data points was calculated during model training; importance1 = T: This parameter indicated that feature importance was calculated, with other parameters set to default.[17] Support vector machine is a supervised learning method mainly used for classifi ation and regression analysis, it is a binary classifi ation model that maps the feature vectors of instances to some points in space. The goal of SVM is to draw a line that "best" separates these 2

classes of points, so that if a new point is introduced later, this line can still make a good classifi ation. Support vector machine is suitable for medium- to small-sized datasets, nonlinear, and high-dimensional classifi ation problems. For the SVM model, we seted kernel = "linear," specifying that the type of kernel function was a linear kernel, with other parameters set to default.[18,19] To assess whether these genes were associated with STEMI, these 3 machine learning analyses were performed in the GSE60993 dataset, and used K-fold cross-validation, where K = 2. The sample grouping (STEMI and Normal) was used as the response variable, the DE-SRGs with diagnostic values were used as the explanatory variable, and "DALEX" package (version 2.4.2) was used to analyze the 3 models to plot residual maps and obtain the optimal model with the minimum sample residual. Moreover, the DE-SRGs in the optimal model were regarded as biomarkers, and their expressions were analyzed in GSE60993 and visualized by a heatmap.

To evaluate the diagnostic efficiency of the diagnostic model composed of biomarkers, the logistic regression analysis was employed on it in GSE60993 (STEMI and Normal) and a ROC curve was plotted. Furthermore, based on multiple logistic regression, "RMS" package was utilized to establish a nomogram, which was subsequently validated by plotting the calibration curve and DCA curve.

In order to validate the diagnostic model, GSE62646 (14 controls, 28 STEMI samples) was used as the external validation data set to plot a ROC curve of biomarkers. Additionally, the expressions of biomarkers were compared between STEMI samples and controls in GSE60993 and GSE62646 through the rank sum test.

Gene Set Enrichment Analysis

In order to further explore the pathways related to the biomarkers, the samples in GSE60993 were divided into high- and low-expression groups according to the median expression of the biomarkers.The differences between the high- and low-expression groups were calculated, and the logFC value of each gene was obtained. According to the logFC value, the genes were ranked from high to low. The sorted genes were used as the gene set to perform KEGG pathway enrichment analysis.

Immune Infilt ation Analysis

CIBERSORT algorithm was applied to compute the proportions of 22 types of immune cells in each sample in GSE60993 dataset. Moreover, the percentage of each type of immune cell was compared between STEMI samples and controls, and $P < .05$ was the statistical signifi ant threshold. The correlation between immune cells and biomarkers was calculated using the R package "psych" (version 2.1.9) and demonstrated by ggploy2 (version 3.3.5). The correlation between biomarkers and different immunomodulators was further analyzed, which aimed to further explore the way biomarkers regulate the immune microenvironment.[20]

Construction of a Competing Endogenous RNA Network

Firstly, the target micro RNA (miRNA) of biomarkers was predicted through the miRDB and miRWalk databases, and the predicted miRNAs from each database were overlapped to obtain the intersected miRNAs as the target miRNAs of biomarkers. Then, the target long non-coding RNAs (lncRNAs) of the target miRNAs were predicted through StarBase. Finally, Cytoscape (version 3.8.2)[21] was used to map the lncRNA–miRna biomarker network.

Drug Prediction and Molecular Docking

The target drug or molecular compounds of biomarkers were predicted on DrugBank database and visualized by Cytoscape as well. The predicted drugs were searched in the FDA drugs database (https://www.drugfuture.com/fda/) to screen for FDA-approved drugs, and the molecular structures of biomarkers and target proteins were obtained from the PubChem and PDB databases. Finally, Docking simulations were performed via AutoDock Vina (version 1.5.7)[22] to generate docking energy, and PyMOL software was performed to visualize the docked complexes. The crystal structures of the biomarkers in the molecular docking with the highest energy were downloaded from PDB database.

Statistical Analyses

For all bioinformatics analyses, R language programs were implemented. Differential expression analysis of genes was performed using the R package "limma" with thresholds set as follows: P-value < .05, |log2FC| > 0.5. Heatmaps were generated using the R package "pheatmap." Gene ontology and KEGG pathway enrichment analysis was performed to identify their common functions and related pathways, with a threshold of P-value < .05. Receiver operating characteristic curves were constructed to assess the diagnostic efficiency of DESenes for STEMI, with an AUC > 0.85. Receiver operating characteristic curves were also constructed to evaluate the diagnostic efficiency of a model consisting of 7 biomarkers, with an overall AUC value exceeding 0.9. A nomogram was constructed using multivariate logistic regression via the "RMS" package, and calibration curves and decision curves were plotted to reflect the predictive ability and clinical applicability of the nomogram. Differential expression box plots of biomarkers were drawn, and the statistical test used was the rank-sum test. The differences in immune cell content between STEMI and normal samples were compared using the rank-sum test. Additionally, the R package "psych" was used to calculate the correlation between immune cells and biomarkers, with a threshold of P-value < .05.

Data Availability

The datasets generated and analyzed during the current study are available in the GEO and CellAge database (https://www.ncbi.nlm.nih.gov/geo/ and http://genomics.senescence.info/cells).

RESULTS

Functional Annotation of 21 Differentially Expressed Cellular Senescence–Related Genes

Among the 17 STEMI samples and 7 controls in GSE60993, 975 DEGs were screened out, including 585 upregulated and 390 downregulated DEGs (Figure 1A and B). After overlapping with the 279 SRGs, a number of 21 DE-SRGs were obtained, which were HDAC4, PTTG1, CEBPB, AKR1B1, RAF1, MMP9,

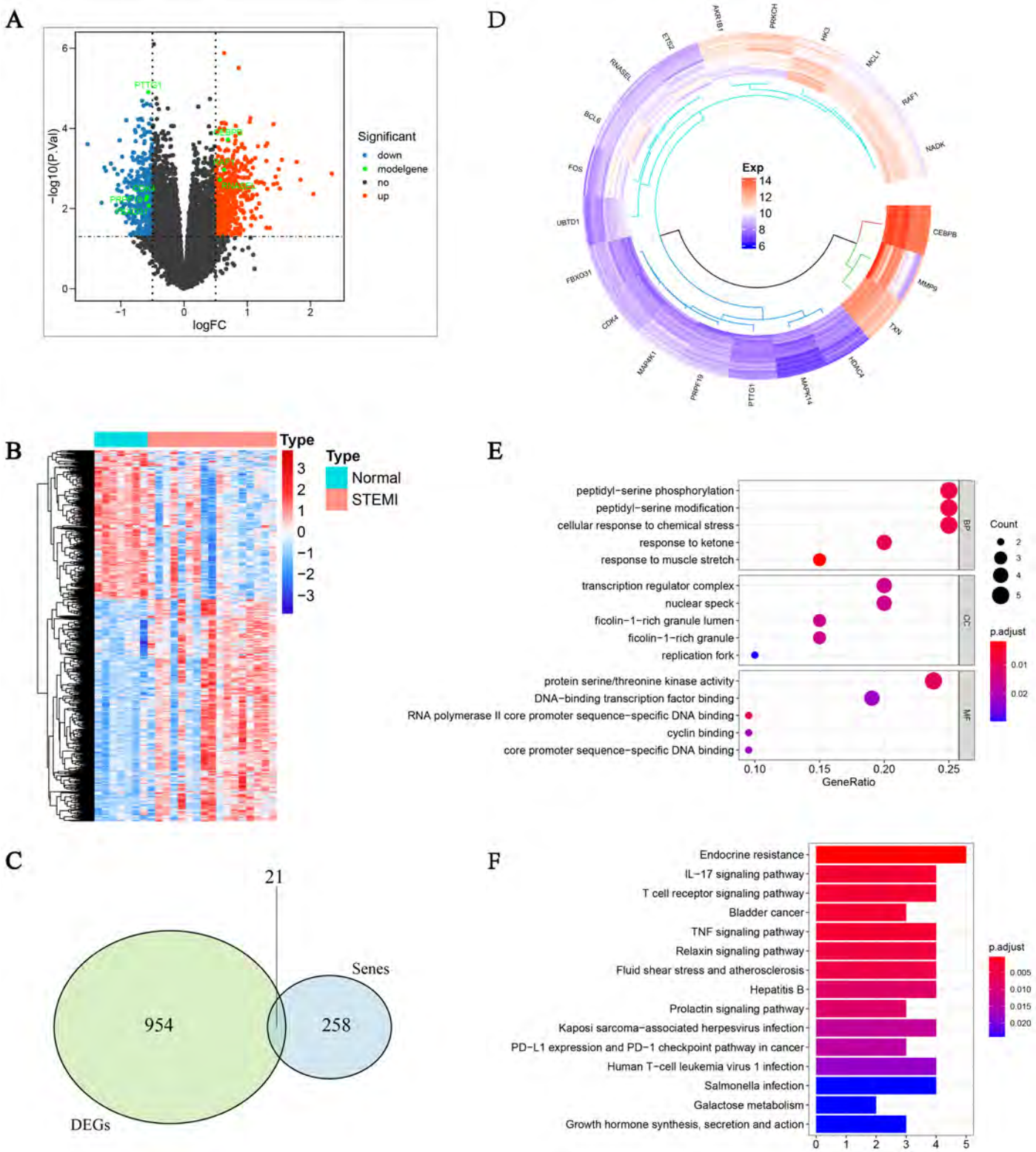

Figure 1. Comprehensive functional annotation of 21 differentially expressed cellular senescence-related genes. (A-B) Volcano map and heatmap showing differentially expressed genes in ST-elevation myocardial infarction and control samples from the 2 gene expression omnibus datasets. (C) Venn diagram of the overlapping genes between differentially expressed genes and senescence-related genes. (D) Heatmap of the 21 differentially expressed cellular senescence-related genes from the integrated analysis. (E) Gene ontology functional enrichment analysis of the 21 differentially expressed cellular senescence-related genes (top 5 terms). (F) Kyoto Encyclopedia of Genes and Genomes revealed the top 15 pathways enriched in the 21 differentially expressed cellular senescence-related genes.

RNASEL, HK3, NADK, UBTD1, FOS, BCL6, CDK4, PRPF19, MCL1, FBXO31, MAP4K1, ETS2, MAPK14, TXN, and PRKCH (Figure 1C). Moreover, it can be found from the expression heat map of DE-SRGs that CEBPB, TXN, and MMP9 were the top 3 DE-SRGs with the highest expression (Figure 1D).

Additionally, based on the selection criteria of $P < .05$, 105 GO terms (95 BP, 5 CC, 5 MF) and 46 KEGG pathways were enriched by 21 DE-SRGs. The dot plot of enriched GO terms showed the top 5 results in each category. For instance, the 21 DE-SRGs were mainly involved in the biological processes of peptidyl–serine phosphorylation, peptidyl–serine modifi ation, cellular response to chemical stress, response to ketones, and response to muscle stretch; the 5 enriched cellular components were transcription regulators complex, nuclear speck, fi olin-1-rich granule lumen, fi olin-1-rich granule, and replication fork; in terms of the 5 molecular functions, they were protein serine/threonine kinase activity, DNA-binding transcription factor binding, RNA polymerase II core promoter sequence–specific DNA binding, cyclin binding, and core promoter sequence–specific DNA binding (Figure 1E). The bar chart showed the top 15 KEGG pathways enriched by 21 DE-SRGs, which mainly included endocrine resistance, interleukin (IL)-17 signaling pathway, T cell receptor signaling pathway, TNF signaling pathway, relaxin signaling pathway, fluid shear stress, and atherosclerosis (Figure 1F).

Seven Biomarkers Were Identifie

The 21 DE-SRGs were initially analyzed by plotting their ROC curves to evaluate their diagnostic values, and 11 of them had an AUC greater than 0.85 and were regarded as DE-SRGs with diagnostic value, which were HDAC4, PTTG1, CEBPB, RAF1, AKR1B1, PRPF19, RNASEL, MMP9, CDK4, HK3, and FBXO31 (Figure 2). Afterward, the residual distribution plots of the 3 machine learning algorithms showed that the SVM was the optimal model, and 7 genes (RAF1, RNASEL, CEBPB, PRPF19, FBXO31, PTTG1, and CDK4) in SVM were the biomarkers of STEMI (Figure 3A). In addition, in the GSE60993 dataset, RAF1, RNASEL, and CEBPB were upregulated in STEMI samples, while the other 4 biomarkers were downregulated (Figure 3B).

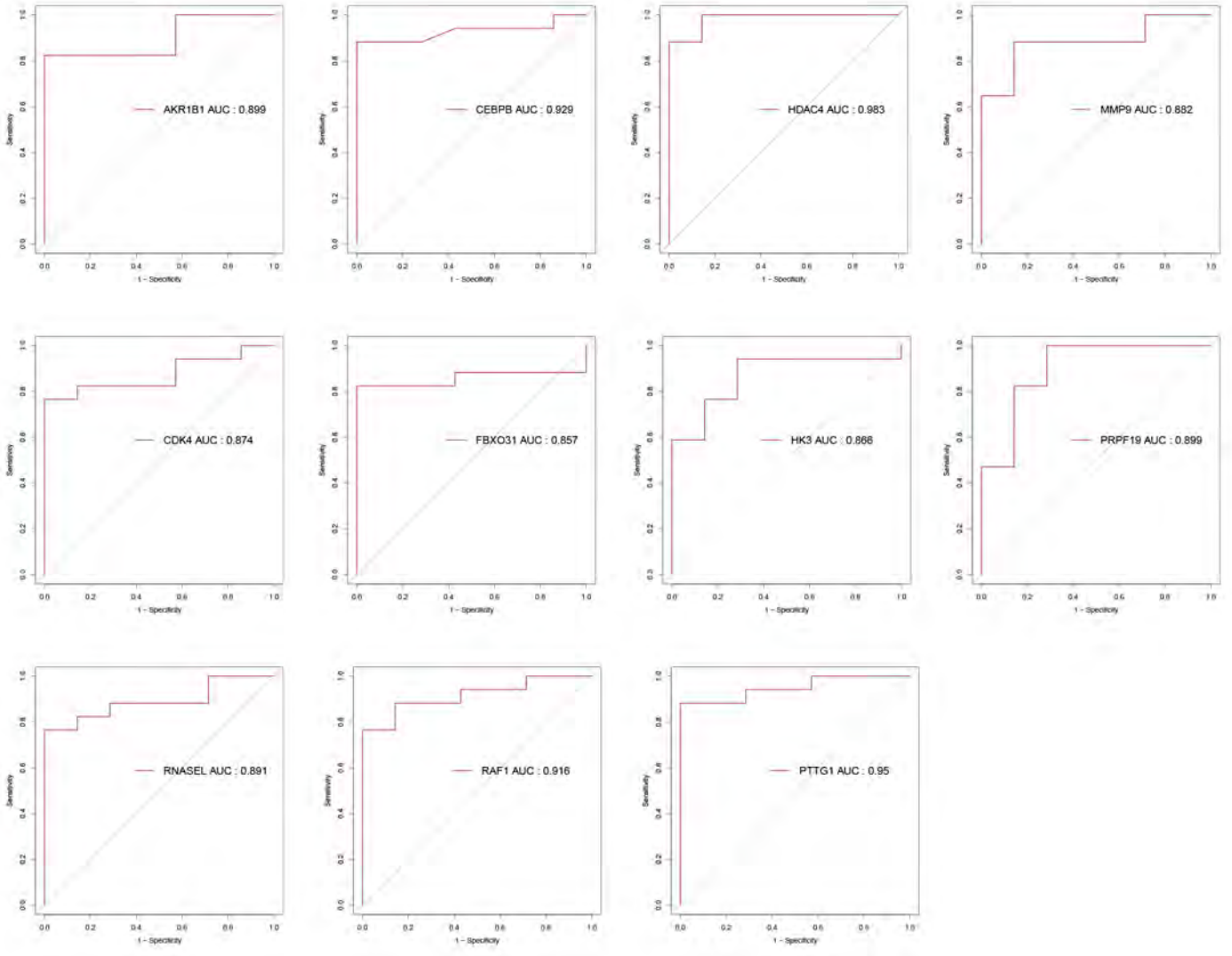

Figure 2. The single-gene receiver operating characteristic curves of genes with area under curve values greater than 0.85.

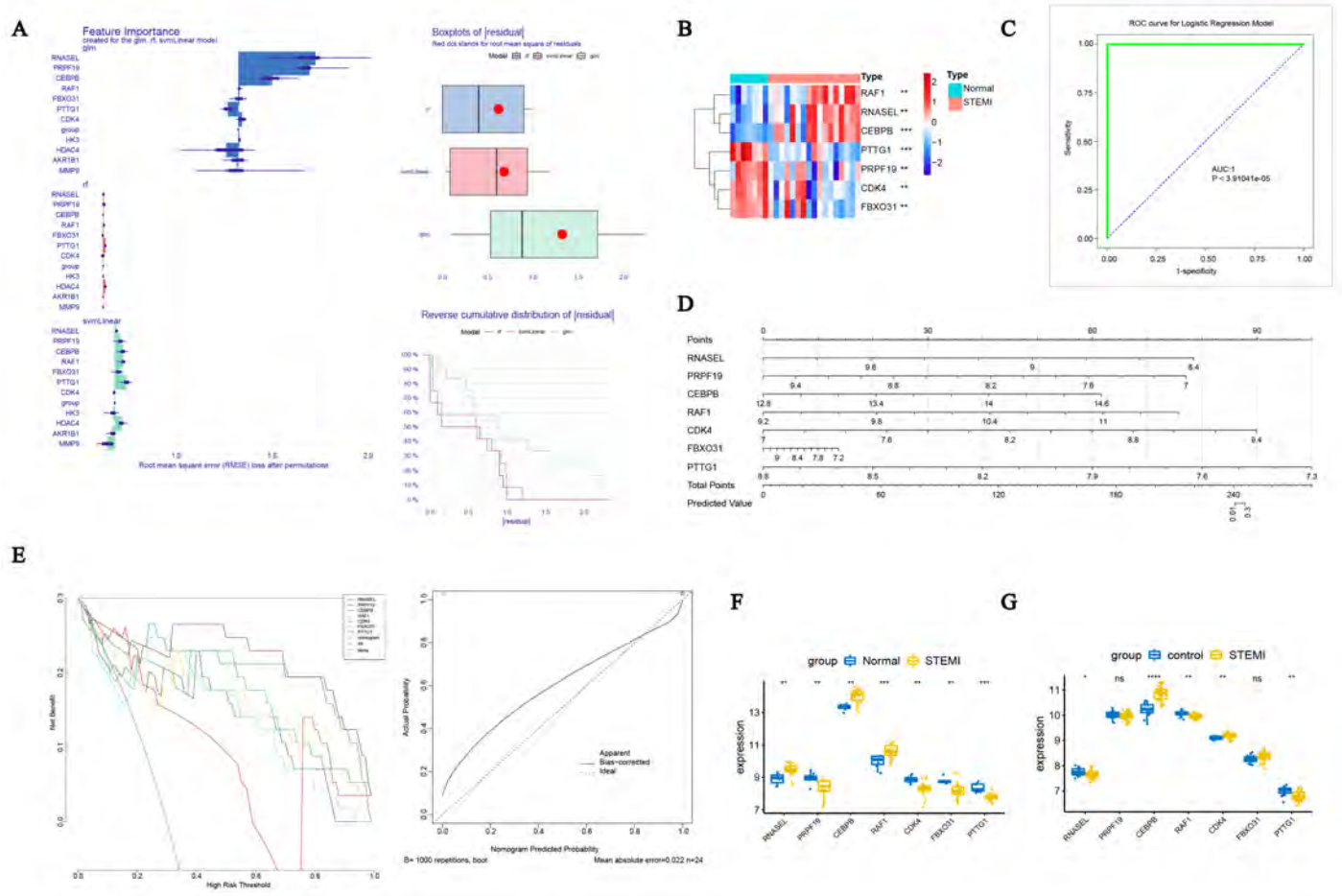

Figure 3. Seven cellular senescence-related biomarkers were identified. (A) The residual distribution plots of the 3 machine learning algorithms. (B) Heatmap of the 7 genes from the support vector machine analysis. (C) The receiver operating characteristic curves of the 7 senescence-related biomarkers as a whole in logistic regression model. (D) Nomogram comprised of the 7 cellular senescence-related biomarkers. (E) DCA curves and calibration curves for the nomogram. (F-G) The expression of 7 cellular senescence-related biomarkers in GSE60993 and GSE62646 cohort.

To further validate the diagnostic efficiency of the 7 biomarkers, a ROC curve of them in GSE60993 was plotted, and the AUC was 1, which indicated that the diagnosis of the biomarkers was accurate (Figure 3C). Moreover, a nomogram consisting of 7 biomarkers was established. The slope of the nomogram calibration curve was close to 1, and the net benefit of the nomogram was the highest compared with other single biomarkers, which all revealed the prediction of the nomogram was accurate (Figure 3D and E).

Furthermore, the ROC validation results of the biomarkers in GSE62646 demonstrated that the AUC of the 7 biomarkers was 1, which was higher than any other single biomarker, illustrating that the diagnostic accuracy of the model was accurate (Supplementary Figure 1A and B).

Finally, it can be found from the biomarker expression comparison in GSE60993 that RNASEL, CEBPB, and RAF1 were expressed signifi antly higher in STEMI samples, whereas the expressions of PRPF19, FBXO31, PTTG1, and CDK4 were distinctly higher in the controls (Figure 3F). On the other hand, in GSE62646, CEBPB and CDK4 were expressed higher in STEMI samples, while RNASEL, RAF1, and PTTG1 were highly expressed in controls (Figure 3G).

Gene Set Enrichment Analysis

To further detect the KEGG pathways related to biomarkers, GSEA was employed on high and low biomarker expression groups. It can be observed that the ribosome was the common pathway of the 7 biomarkers, and except for PRPF19, the remaining 6 biomarkers all enriched the autophagy animal pathway. Additionally, allograft rejection was the common pathway enriched by CDK4, FBXO31, PRPF19, and RAF1. Autoimmune thyroid disease is the common pathway of CDK4, FBXO31, and PRPF19. Moreover, CDK4, CEBPB, FBXO31, and RAF1 were commonly enriched in complement and coagulation cascades (Figure 4).

Immune Infilt ation Analysis

The CIBERSORT result of GSE60993 indicated that monocytes accounted for a larger ratio in the majority of samples (Figure 5A). It can be clearly seen from the comparison results that CD4 memory T cells activated and gamma delta T cells represented signifi antly higher proportions in normal

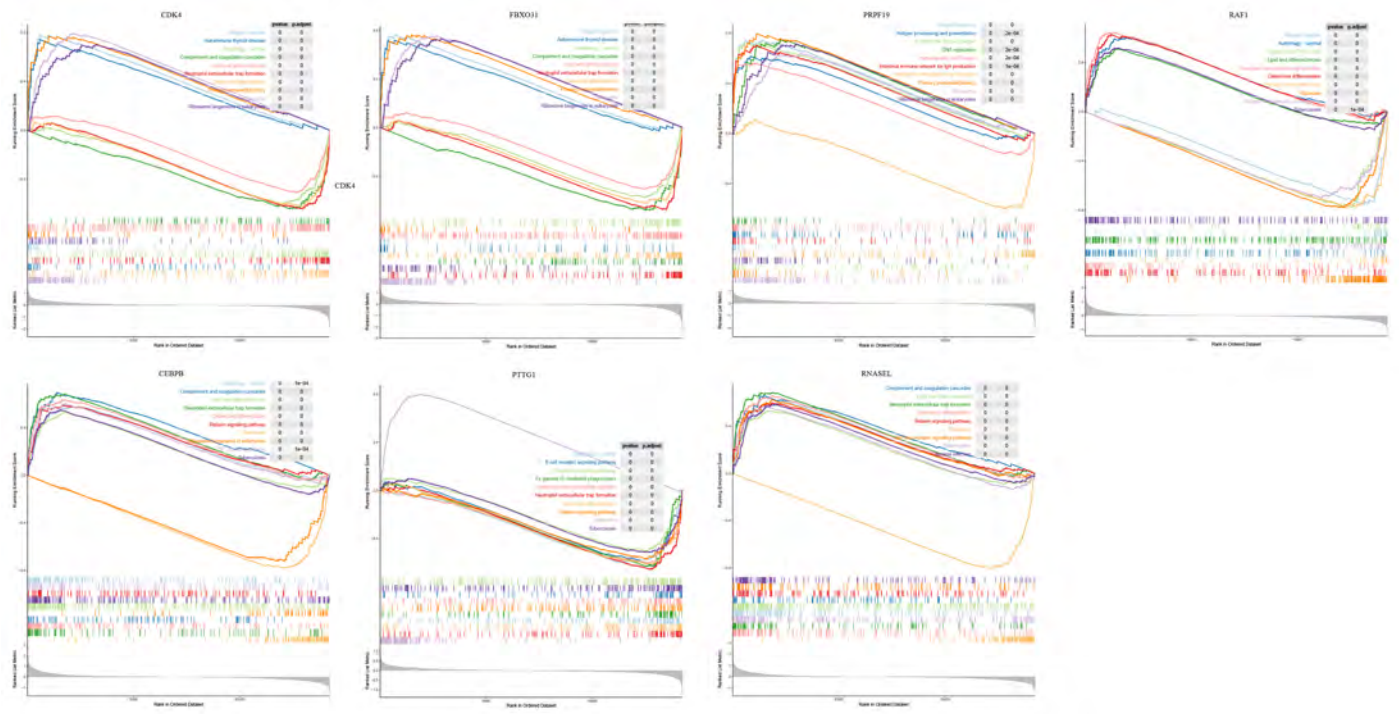

Figure 4. Gene set enrichment analysis annotation of the 7 cellular senescence-related biomarkers.

samples compared to STEMI samples, while the rates of monocytes and neutrophils were distinctly higher in STEMI samples (Figure 5B).

The correlations between biomarkers and the immune cells in GSE60993 showed that a signifi antly positive correlation was found between CEBPB and Monocytes ($r = 0.789$, $P < .001$), CEBPB and neutrophils ($r = 0.708$, $P < .001$), and FBXO31 and CD8 T cells CD8 ($r = 0.735$, $P < .001$). The signifi antly negative correlation was between CEBPB and T cells, CD8 ($r = -0.704$, $P < .001$), and FBXO31 and monocytes ($r = -0.753$, $P < .001$) (Figure 5C).

Furthermore, the correlations between biomarkers and immunomodulators demonstrated that the strongest positive correlation existed between FBXO3 and CD40LG (0.872), followed by a correlation between FBXO3 and LTA (0.853), and a correlation between FBXO3 and TNFRSF25 (0.852). On the other hand, the most negative correlations were between FBXO3 and ENTPD1 (−0.886), followed by the correlation between FBXO3 and IL10RB (−0.844), and the correlation between CDK4 and ENTPD1 (−0.838) (Figure 5D).

Competing Endogenous RNA Network Construction

A number of 15 common target miRNAs were obtained from the overlap analysis between 307 miRNAs from miRDB and 59 miRNAs from miRWalk (Figure 6A). Subsequently, the target lncRNAs could be predicted by 9 miRNAs (hsa-miR-6783-3p, hsa-miR-3622b-5p, hsa-miR-3194-3p, hsa-miR-519d-3p, hsa-miR-497-5p, hsa-miR-423-5p, hsa-miR-93-5p, hsa-miR-20a-5p, and hsa-miR-17-5p) from StarBase, and a lncRNA-miRNA-Biomarker network comprising 281 nodes and 563 edges was constructed (Figure 6B). For instance, AP003419.2 could regulate CDK4, CEBPB, and FBXO31 through hsa-miR-3622b-5p, and OLMALINC could regulate FBXO31 through hsa-miR-17-5p.

Drug Prediction and Molecular Docking

A total number of 16 drugs (Table 1) were predicted through DrugBank by 4 biomarkers (RNASEL, CEBPB, RAF1, CDK4) (Figure 7A). It can be found that Fostamatinib was the common target drug for RAF1 and CDK4, and only 1 drug was predicted by RNASEL and CEBPB, which was 2′-Deoxyuridine 3′-Monophosphate and Quercetin respectively.

Moreover, the Autodock Vina results revealed that the docking energy of Regorafenib-RAF1 and Fostamatinib-CDK4 was the highest (−7.1) (Figure 7C and D). The 3D conformer structure diagrams of Regorafenib and Fostamatinib were displayed in Figure 7B. Subsequently, the visualized result of Regorafenib-RAF1 by PyMOL showed that the LEU-149 residue had a hydrogen bond interaction with the Regorafenib molecule. The docking affinity between the active molecule and the protein was −7.1 kcal/mol. Additionally, it can be seen from the Fostamatinib-CDK4 docking that hydrogen bond interactions existed between Fostamatinib and the residues (ARG37 and ARG41), and the docking affinity between the active molecule and the protein was −7.1 kcal/mol (Figure 7C and D).

DISCUSSION

ST-elevation myocardial infarction remains a leading cause of premature death worldwide, with an estimated 1.5 million cases annually in the United States alone.[23] Recent research has highlighted the role of cellular senescence in the pathogenesis of STEMI. Histone acetylation, lower global DNA methylation levels, and shorter telomere length have been

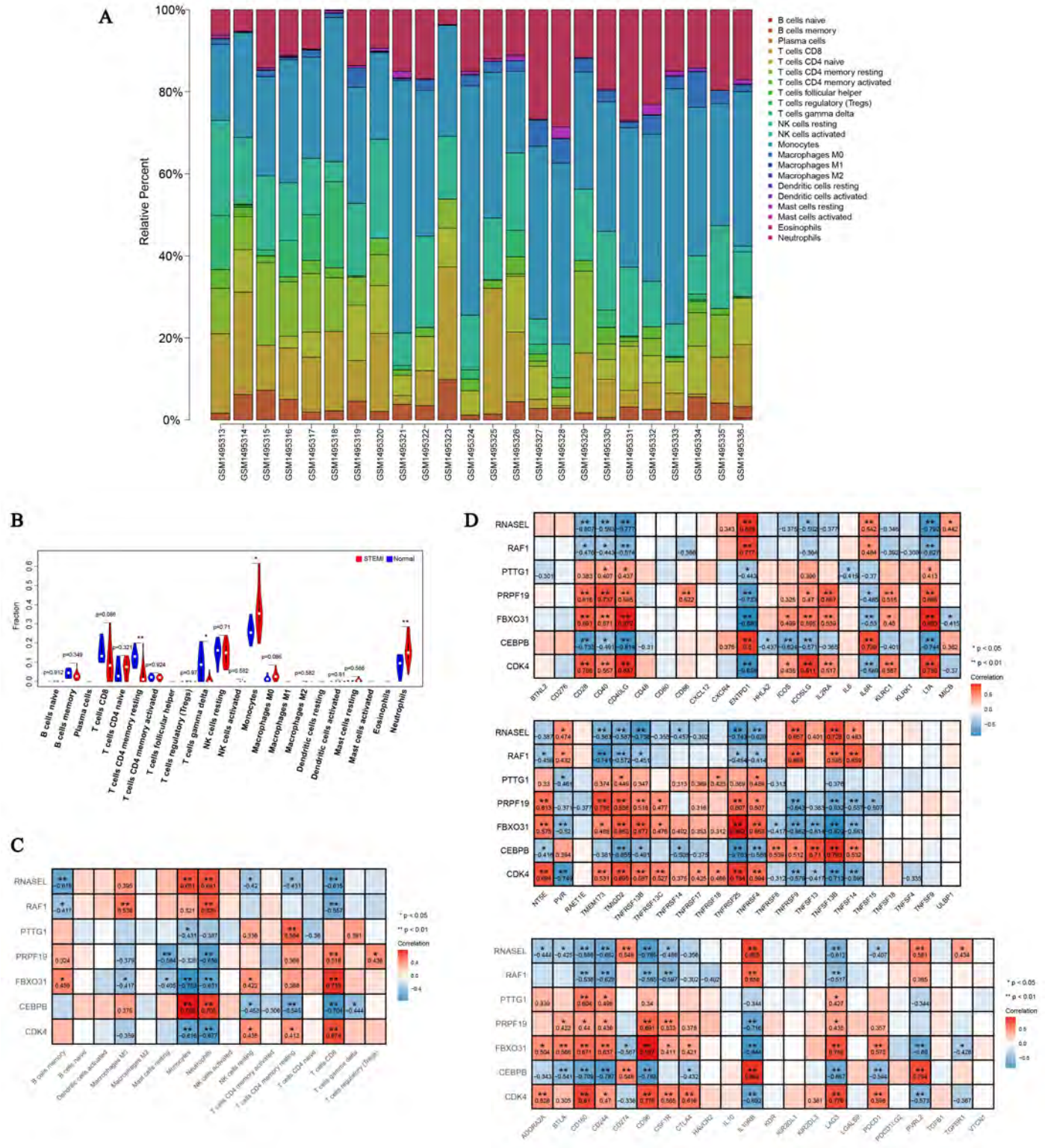

Figure 5. Estimation of infilt ating immune cell types in GSE60993 cohort via CIBERSORT. (A) Stacked bar plot showing the relative composition of 22 immune cell subsets in the cohort. (B) The violin diagram shows the immune cell difference between normal and differentially expressed cellular senescence-related genes samples. (C) Correlation analysis of the 7 cellular senescence-related biomarkers and different immune cell types. (D) Correlation analysis of the 7 cellular senescence-related biomarkers with immunosuppressive and immunostimulatory factors. *$P < .05$, **$P < .01$.

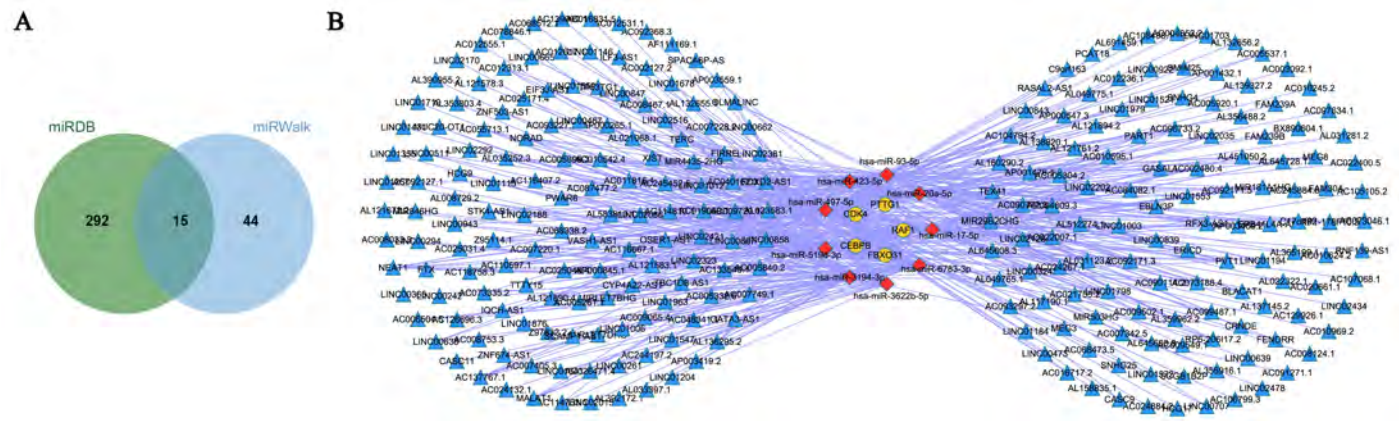

Figure 6. Prediction of the micro RNA–messenger RNA network and competing endogenous RNA network. (A) Venn diagram of the overlapping micro RNAs from the miRDB and miRWalk databases; (B) the long non-coding RNA–micro RNA network includes CDK4, CEBPB, FBXO31, RAF1, and PRPF19.

associated with an increased risk of cardiovascular disease, including STEMI.[24] Therefore, exploring the changes of cellular senescence genes in STEMI may provide a new direction for future treatment of STEMI.

Peptidyl–serine phosphorylation and modifi ation are known to play a critical role in cellular signaling pathways that regulate various cellular processes, including the cellular response to chemical stress, response to ketones, and response to muscle stretch. A study found that peptidyl–serine phosphorylation of the stress-induced protein HSP27 regulates the cellular response to chemical stress by promoting cell survival and preventing apoptosis.[25] Another study published in the Journal of Neurochemistry demonstrated that peptidyl–serine modifi ation of the ketone body β-hydroxybutyrate regulates its transport across the blood-brain barrier and plays a role in the response to ketones.[26] Additionally, a study published in the Journal of Applied Physiology showed that peptidyl–serine modifi ation of the extracellular matrix protein tenascin-C is involved in the response to muscle stretch and the regulation of muscle adaptation.[27] Peptidyl–serine phosphorylation has been implicated in the pathophysiology of STEMI based on the signifi ant elevation of serum levels of the cardiac troponin I marker for peptidyl–serine phosphorylation in STEMI patients.[28] Consistent with previous reports, this present study found that 21 DE-SRGs were enriched in these biological processes. Furthermore, this study identified an association between cellular SRGs and key cellular processes, such as protein serine/threonine kinase activity, DNA-binding transcription factor binding, sequence-specific DNA binding, cyclin binding, and core promoter sequence-specific DNA binding. These processes have been previously linked to various cellular functions, and their dysregulation may contribute to the pathogenesis of STEMI.[29] We also identified 21 DE-SRGs that exhibit a strong correlation with Relaxin signaling, fluid shear stress, and atherosclerosis. The authors' findings suggest that these pathways have signifi ant implications in the development of STEMI, as they promote angiogenesis, regulate endothelial cell function, and maintain vascular homeostasis.[30] Besides, endocrine resistance, IL-17 signaling pathway, T cell receptor signaling pathway, and TNF signaling pathway correlated with STEMI, suggesting that they may be involved in STEMI by regulating infla - matory and immune signaling pathways. Understanding the interplay between these pathways and their contribution to the pathogenesis of STEMI may provide new insights into the therapies for the prevention and treatment of this condition.

While the Fourth Universal Definition of Myocardial Infarction offers a refined framework for diagnosing and assessing STEMI, distinguishing myocardial ischemia from conditions like pulmonary embolism or hypertrophic cardiomyopathy remains challenging in complex cases.[31] For instance, high-sensitivity cardiac troponin, detectable within 2-4 hours of ischemia, aids diagnosis but can also rise due to non-ischemic factors like mechanical stress.[32] Thus, more specific biomarkers are needed to improve diagnostic accuracy. The authors' research has revealed a signifi ant upregulation of RAF1 and CEBPB in the context of STEMI, which aligns with previous studies confirming the involvement of RAF1 and CEBPB in the pathophysiological processes of myocardial infarction.[33,34] Furthermore, the authors' analysis revealed bidirectional expression of RNASEL in this clinical context across different databases, suggesting that innate immune responses may play a signifi ant role in the progression of STEMI.[35] Notably, we observed the downregulation of PRPF19 and FBXO31 in STEMI. Although the direct relationship between these 2 factors and STEMI has not yet been clarified, considering the critical role of PRPF19 in messenger RNA (mRNA) maturation and processing, as well as the important regulatory functions of FBXO31 in protein degradation and DNA stability, it is speculated that they may exert similar regulatory effects in STEMI.[36,37] PTTG1 and CDK4, as key factors in maintaining chromosomal stability, have been shown by recent evidence to be involved in the regulation of myocardial hypertrophy and cellular regeneration following myocardial infarction, further highlighting their potential roles in STEMI.[38,39] Notably, we observed contradictory outcomes for PTTG1 and CDK4 in STEMI samples across various databases. The authors' hypothesis is that the observed phenomenon may be associated with the extent of myocardial injury,

Table 1. Drugs Prediction of RNASEL, CEBPB, RAF1, and CDK4 by DrugBank

DrugBank ID	Name	Drug Group	Pharmcological Action	Actions	Gene
DB03448	2′-Deoxyuridine 3′-Monophosphate	Experimental			*RNASEL*
DB00398	Sorafenib	Aapproved, investigational	Yes	Inhibitor	*RAF1*
DB04973	LErafAON	Investigational	Unknown		*RAF1*
DB05268	iCo-007	Investigational	Unknown		*RAF1*
DB05190	XL281	Investigational	Unknown		*RAF1*
DB08896	Regorafenib	Approved	Yes	Inhibitor	*RAF1*
DB08912	Dabrafenib	Approved, investigational	Yes	Inhibitor	*RAF1*
DB08862	Cholecystokinin	Approved, investigational	Unknown	Agonist	*RAF1*
DB12010	Fostamatinib	Approved, investigational	Unknown	Inhibitor	*RAF1*
DB04216	Quercetin	Experimental, investigational			*CEBPB*
DB03496	Alvocidib	Experimental, investigational	Unknown		*CDK4*
DB02733	Purvalanol	Experimental	Unknown		*CDK4*
DB09073	Palbociclib	Approved, investigational	Yes	Inhibitor	*CDK4*
DB11730	Ribociclib	Approved, investigational	Yes	Antagonistinhibitor	*CDK4*
DB12001	Abemaciclib	Approved, investigational	Yes	Inhibitor	*CDK4*
DB12010	Fostamatinib	Approved, investigational	Unknown	Inhibitor	*CDK4*
DB15442	Trilaciclib	Approved, investigational	Yes	Inhibitor	*CDK4*

as it involves various vessels and blood cells.[40] We found that biological pathways such as autophagy, the complement system, and the coagulation cascade are all involved in the entire process of inflamma ory responses in myocardial infarction.[41,42] This finding is highly consistent with the GSEA analysis of the 7 biomarkers identified in this tudy.

Since the model in this study was constructed using a dataset exclusively comprising samples collected within 4 hours of symptom onset or on the day of admission, these 7 biomarkers may possess unique risk assessment value for untreated and high-risk STEMI patients. However, whether these biomarkers also exhibit signifi ant changes in other stages of STEMI (such as the acute, subacute, and chronic phases) still requires further in-depth investigation. By conducting continuous blood tests to evaluate the expression patterns of these markers across different stages of STEMI—from early injury phase to healing phase—critical insights may be gained into their roles in disease progression, treatment response, and prognostic evaluation. For example, the bidirectional expression of RNASEL and the differential expression patterns of PTTG1 and CDK4 not only enhance the ability to differentiate STEMI from other conditions (e.g., pulmonary embolism or hypertrophic cardiomyopathy) but also provide valuable insights into the severity of myocardial injury and the progression of recovery. Additionally, the upregulation of RAF1 and CEBPB in the early stages may serve as sensitive indicators of ongoing ischemic injury, while the downregulation of PRPF19 and FBXO31 in later stages could reflect the extent of myocardial damage and repair processes. By integrating these biomarkers into traditional diagnostic and risk stratifi a-tion models, we anticipate signifi ant improvements in the accuracy of STEMI diagnosis, optimization of risk assessment, and enhanced guidance for clinical decision-making, ultimately leading to better patient outcomes. By integrating these biomarkers into traditional diagnostic and risk stratifi ation models, it is possible to improve the accuracy of STEMI diagnosis, optimize risk assessment, and provide potential clinical benefit .

The acute-phase treatment of STEMI and subsequent long-term care not only impose a signifi ant financial burden on patients' families but also create substantial pressure on the healthcare system.[43] Therefore, advancing early diagnosis and personalized treatment is crucial to reducing patient costs and improving healthcare resource utilization. Although the implementation of continuous blood monitoring for these biomarkers may increase the initial costs of STEMI diagnosis and treatment, these additional expenses are likely to be offset by the clinical benefits they provide. Continuous monitoring of these 7 biomarkers enables earlier and more accurate identifi ation of high-risk patients, thereby optimizing treatment strategies and reducing unnecessary medical interventions and hospital stays. Furthermore, the potential of these biomarkers in assessing the extent of myocardial injury and predicting prognosis may help reduce the incidence of long-term complications associated with STEMI, such as heart failure and reinfarction, thereby decreasing subsequent healthcare resource utilization.[44] In the long term, this precision medicine approach is expected to improve diagnostic and therapeutic efficienc , enhance patient outcomes, and ultimately reduce overall healthcare costs. Therefore, while the initial investment may be higher, the potential economic benefits and societal value warrant further exploration and validation.

CIBERSORT analysis revealed that CD4 memory T cells and gamma delta T cells were signifi antly decreased in STEMI samples, indicating the long-term protection against

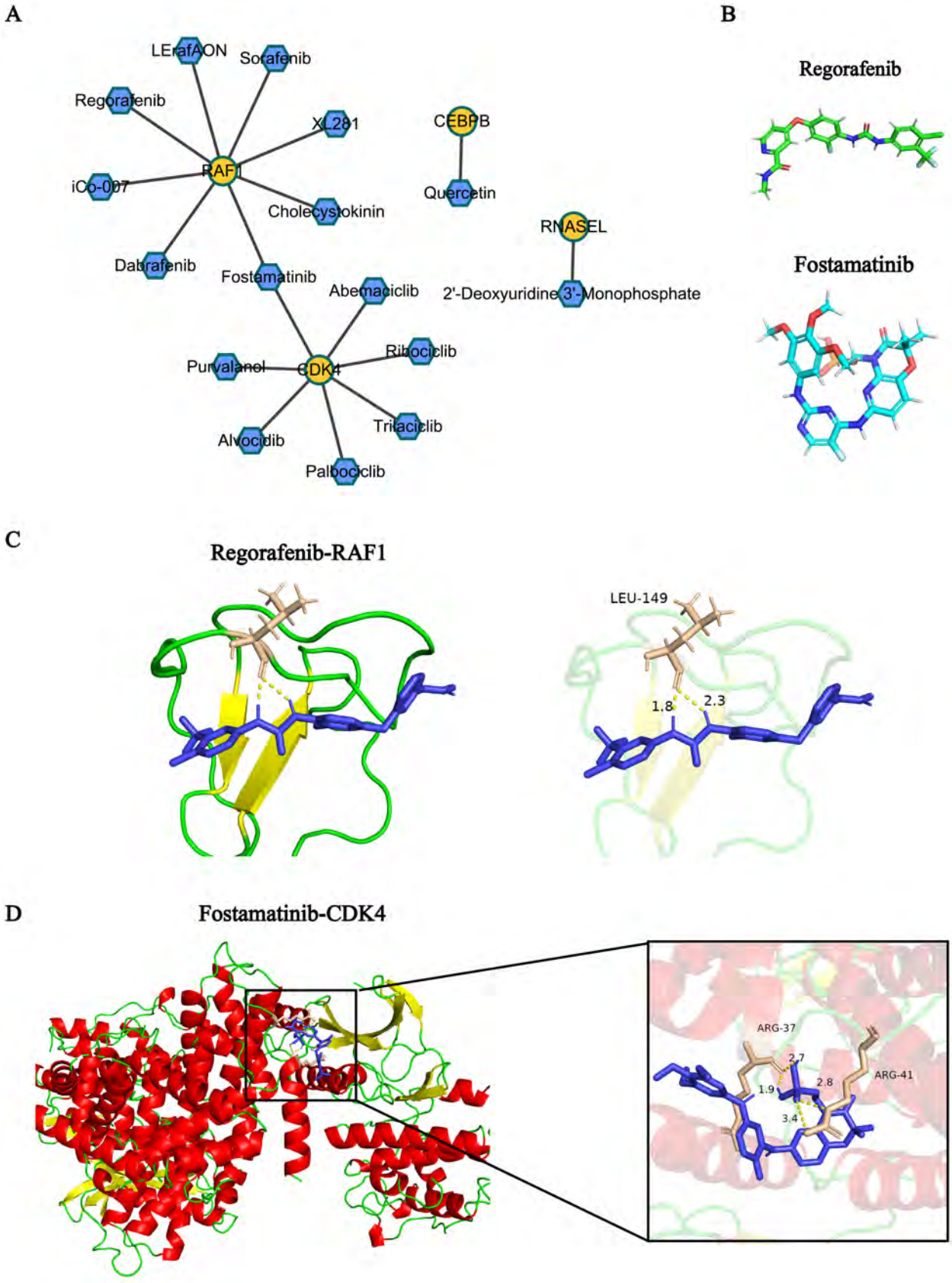

Figure 7. Drug prediction and molecular docking. (A) Drug prediction of *RNASEL*, *CEBPB*, *RAF1*, and *CDK4*; (B) conformer structure diagrams of Regorafenib and Fostamatinib; (C) molecular docking of Regorafenib and *RAF1*; (D) molecular docking of Fostamatinib and *CDK4*.

pathogens and the maintenance of immunological memory were impaired.[45] Conversely, an elevation in monocytes and neutrophils, which have been implicated in the development of inflamma ory diseases, was observed in patients with STEMI, suggesting that the identified biomarkers may modulate the inflamma ory response in the context of STEMI.[46] Furthermore, a central role of RAF1, CDK4, CEBPB, FBXO31, and PTTG1 in the regulation of STEMI was determined. We predicted a ceRNA network of 9 miRNAs (hsa-miR-6783-3p, hsa-miR-3622b-5p, hsa-miR-3194-3p, hsa-miR-519d-3p, hsa-miR-497-5p, hsa-miR-423-5p, hsa-miR-93-5p, hsa-miR-20a-5p, and hsa-miR-17-5p) in the regulation of RAF1, CDK4, CEBPB, FBXO31, and PTTG1, providing new avenues for combination targeted therapy in STEMI.

Through this predictive analyses of the interactions between drug molecules and the 7 biomarkers, we identified RAF1 and CDK4 inhibitors as potentially effi acious therapeutics for STEMI. Cholecystokinin has demonstrated a capacity to reduce myocardial fib osis and improve cardiac remodeling in animal models.[47] Nevertheless, Regorafenib, another RAF1 inhibitor, has been reported to induce hypertension and myocardial ischemia in a patient with gastrointestinal stream tumors.[48] It is possible that the observed effect can be attributed to the multitargeted nature of Regorafenib, which inhibits a diverse array of kinases such as VEGFR1-3, PDGFR-beta, and RTKs.[49] Other study has found that CEBPB-related drug, quercetin reduces the expression of inflamma ory factors, increases total antioxidant capacity, and improves quality of life in patients following myocardial infarction.[50] In further, it is imperative to focus on the development of novel drug-related interventions to effectively manage STEMI.

The present study provides support for the involvement of candidate genes and functional pathways in cellular senescence-related STEMI. Previous studies have utilized gene expression analysis for the examination of STEMI,[51] but none have specifi ally focused on cellular senescence. Additionally, given the variability in treatment methods and timing, it can be challenging to isolate molecular mechanisms that are solely attributable to STEMI. Hence, future research should concentrate on validating the roles of candidate gene signaling axis pathways that potentially mediate cellular senescence-related STEMI. The complexity of the STEMI mechanism is compounded by the limited use of drugs in clinical or animal research, which were not further validated in this study.[47] Despite the absence of experimental verifi ation, the findings provide a solid foundation for guiding clinical and experimental research related to cellular senescence-related STEMI.

CONCLUSION

Through a comprehensive suite of bioinformatics analyses, several prominent candidate genes, including *RAF1, RNASEL, CEBPB, PRPF19, FBXO31, PTTG1,* and *CDK4*, were identified alongside multiple enriched functional signaling pathways that may be involved in the pathogenesis of cellular senescence-induced STEMI.

Data Availability Statement: This manuscript did not produce new data; all pertinent data were described in the Methods section and were sourced from GEO datasets.

Ethics Committee Approval: This article does not involve any research or experimental data or other information related to human or animal subjects.

Peer-review: Externally peer reviewed.

Author Contributions: Liya Li, as the fir t author, analyzed, organized, and processed the GEO dataset samples and completed the original draft manuscript; Pei Qin designed, reviewed, and revised the manuscript; Pei Qin and Liya Li administrated the project and provided the funding. All authors contributed to the article and approved the submitted version.

Declaration of Interests: The authors have no conflicts of interest to declare.

Funding: This study was supported by grant from the National Natural Science Foundation of China (81901205, 82401743).

Statement on Use of AI-Assisted Technologies: No AI-assisted technologies, such as Large Language Models (LLMs), chatbots, or image creators, were utilized in the production of this manuscript.

REFERENCES

1. Bhatt DL, Lopes RD, Harrington RA. Diagnosis and treatment of acute coronary syndromes: a review. *JAMA*. 2022;327(7):662-675. [CrossRef]
2. Choudhury T, West NE, El-Omar M. ST elevation myocardial infarction. *Clin Med (Lond)*. 2016;16(3):277-282. [CrossRef]
3. Towashiraporn K. Current recommendations for revascularization of non-infarct-related artery in patients presenting with ST-segment elevation myocardial infarction and multivessel disease. *Front Cardiovasc Med*. 2022;9:969060. [CrossRef]
4. Harrington DH, Stueben F, Lenahan CM. ST-elevation myocardial infarction and non-ST-elevation myocardial infarction: medical and surgical interventions. *Crit Care Nurs Clin North Am*. 2019;31(1):49-64. [CrossRef]
5. Vogel B, Claessen BE, Arnold SV, et al. ST-segment elevation myocardial infarction. *Nat Rev Dis Primers*. 2019;5(1):39. [CrossRef]
6. Ibanez B, James S, Agewall S, et al. 2017 ESC Guidelines for the management of acute myocardial infarction in patients presenting with ST-segment elevation: the Task Force for the management of acute myocardial infarction in patients presenting with ST-segment elevation of the European Society of Cardiology (ESC). *Eur Heart J*. 2018;39(2):119-177. [CrossRef]
7. Farhadnejad H, Emamat H, Zand H. The effect of resveratrol on cellular senescence in normal and cancer cells: focusing on cancer and age-related diseases. *Nutr Cancer*. 2019;71(7):1175-1180. [CrossRef]
8. Li Z, Zhang Z, Ren Y, et al. Aging and age-related diseases: from mechanisms to therapeutic strategies. *Biogerontology*. 2021;22(2):165-187. [CrossRef]
9. Childs BG, Baker DJ, Wijshake T, Conover CA, Campisi J, van Deursen JM. Senescent intimal foam cells are deleterious at all stages of atherosclerosis. *Science*. 2016;354(6311):472-477. [CrossRef]
10. Chen MS, Lee RT, Garbern JC. Senescence mechanisms and targets in the heart. *Cardiovasc Res*. 2022;118(5):1173-1187. [CrossRef]
11. Antelo-Iglesias L, Picallos-Rabina P, Estévez-Souto V, Da Silva-Álvarez S, Collado M. The role of cellular senescence in tissue

repair and regeneration. *Mech Ageing Dev*. 2021;198:111528. [CrossRef]
12. Avelar RA, Ortega JG, Tacutu R, et al. A multidimensional systems biology analysis of cellular senescence in aging and disease. *Genome Biol*. 2020;21(1):91. [CrossRef]
13. Xu M, Kong Y, Chen N, et al. Identifi ation of immune-related gene signature and prediction of CeRNA network in active ulcerative colitis. *Front Immunol*. 2022;13:855645. [CrossRef]
14. Phipson B, Lee S, Majewski IJ, Alexander WS, Smyth GK. Robust hyperparameter estimation protects against hypervariable genes and improves power to detect differential expression. *Ann Appl Stat*. 2016;10(2):946-963. [CrossRef]
15. Wu T, Hu E, Xu S, et al. clusterProfiler 4.0: a universal enrichment tool for interpreting omics data. *Innovation (Camb)*. 2021;2(3):100141. [CrossRef]
16. Gorriz JM, Jimenez-Mesa C, Segovia F, Ramirez J, Suckling J. A connection between pattern classification by machine learning and statistical inference with the General Linear model. *IEEE J Biomed Health Inform*. 2022;26(11):5332-5343. [CrossRef]
17. Hu J, Szymczak S. A review on longitudinal data analysis with random forest. *Brief Bioinform*. 2023;24(2):bbad002. [CrossRef]
18. Kourou K, Exarchos TP, Exarchos KP, Karamouzis MV, Fotiadis DI. Machine learning applications in cancer prognosis and prediction. *Comput Struct Biotechnol J*. 2015;13:8-17. [CrossRef]
19. Huang S, Cai N, Pacheco PP, Narrandes S, Wang Y, Xu W. Applications of support vector machine (SVM) learning in cancer genomics. *Cancer Genomics Proteomics*. 2018;15(1):41-51. [CrossRef]
20. Shi J, Cavagnaro MJ, Xu S, Zhao M. The application of three-dimensional technologies in the improvement of orthopedic surgery training and medical education quality: a comparative bibliometrics analysis. *Front Bioeng Biotechnol*. 2022;10:852608. [CrossRef]
21. Shannon P, Markiel A, Ozier O, et al. Cytoscape: a software environment for integrated models of biomolecular interaction networks. *Genome Res*. 2003;13(11):2498-2504. [CrossRef]
22. Trott O, Olson AJ. AutoDock Vina: improving the speed and accuracy of docking with a new scoring function, efficie t optimization, and multithreading. *J Comput Chem*. 2010;31(2):455-461. [CrossRef]
23. Benjamin EJ, Muntner P, Alonso A, et al. Heart disease and stroke Statistics-2019 update: a report from the American Heart Association. *Circulation*. 2019;139(10):e56-e528. [CrossRef]
24. Kalea AZ, Drosatos K, Buxton JL. Nutriepigenetics and cardiovascular disease. *Curr Opin Clin Nutr Metab Care*. 2018;21(4):252-259. [CrossRef]
25. Stokoe D, Engel K, Campbell DG, Cohen P, Gaestel M. Identifi ation of MAPKAP kinase 2 as a major enzyme responsible for the phosphorylation of the small mammalian heat shock proteins. *FEBS Lett*. 1992;313(3):307-313. [CrossRef]
26. Robinson AM, Williamson DH. Physiological roles of ketone bodies as substrates and signals in mammalian tissues. *Physiol Rev*. 1980;60(1):143-187. [CrossRef]
27. Flück M, Mund SI, Schittny JC, Klossner S, Durieux AC, Giraud MN. Mechano-regulated tenascin-C orchestrates muscle repair. *Proc Natl Acad Sci U S A*. 2008;105(36):13662-13667. [CrossRef]
28. Antman EM, Tanasijevic MJ, Thompson B, et al. Cardiac-specific troponin I levels to predict the risk of mortality in patients with acute coronary syndromes. *N Engl J Med*. 1996;335(18):1342-1349. [CrossRef]
29. Fujio Y, Matsuda T, Oshima Y, et al. Signals through gp130 upregulate Wnt5a and contribute to cell adhesion in cardiac myocytes. *FEBS Lett*. 2004;573(1-3):202-206. [CrossRef]
30. Souilhol C, Serbanovic-Canic J, Fragiadaki M, et al. Endothelial responses to shear stress in atherosclerosis: a novel role for developmental genes. *Nat Rev Cardiol*. 2020;17(1):52-63. [CrossRef]
31. Bueno H, Rossello X, Bardají A. Has the Fourth Universal Defin tion of myocardial infarction led to better diagnosis and risk stratifi ation? *Eur Heart J*. 2021;42(26):2562-2564. [CrossRef]
32. Thygesen K, Alpert JS, Jaffe AS, et al. Fourth universal defin tion of myocardial infarction (2018). *Eur Heart J*. 2019;40(3):237-269. [CrossRef]
33. Pei J, Cai L, Wang F, et al. LPA(2) contributes to vascular endothelium homeostasis and cardiac remodeling after myocardial infarction. *Circ Res*. 2022;131(5):388-403. [CrossRef]
34. Radmanić L, Korać P, Gorenec L, et al. Distinct expression patterns of genes coding for biological response modifiers involved in inflamma ory responses and development of fib osis in chronic hepatitis C: upregulation of SMAD-6 and MMP-8 and downregulation of CAV-1, CTGF, CEBPB, PLG, TIMP-3, MMP-1, ITGA-1, ITGA-2 and LOX. *Medicina (Kaunas)*. 2022;58(12):1734. [CrossRef]
35. Li Y, Renner DM, Comar CE, et al. SARS-CoV-2 induces double-stranded RNA-mediated innate immune responses in respiratory epithelial-derived cells and cardiomyocytes. *Proc Natl Acad Sci U S A*. 2021;118(16):e2022643118. [CrossRef]
36. He Y, Huang C, Cai K, et al. PRPF19 promotes tongue cancer growth and chemoradiotherapy resistance. *Acta Biochim Biophys Sin (Shanghai)*. 2021;53(7):893-902. [CrossRef]
37. Choppara S, Malonia SK, Sankaran G, Green MR, Santra MK. Degradation of FBXO31 by APC/C is regulated by AKT- and ATM-mediated phosphorylation. *Proc Natl Acad Sci U S A*. 2018;115(5):998-1003. [CrossRef]
38. Levy D, Ferreira MCMR, Reichert CO, et al. Cell cycle changes, DNA ploidy, and PTTG1 gene expression in HTLV-1 patients. *Front Microbiol*. 2020;11:1778. [CrossRef]
39. Abouleisa RRE, Salama ABM, Ou Q, et al. Transient cell cycle induction in cardiomyocytes to treat subacute ischemic heart failure. *Circulation*. 2022;145(17):1339-1355. [CrossRef]
40. Nanni L, Romualdi C, Maseri A, Lanfranchi G. Differential gene expression profiling in genetic and multifactorial cardiovascular diseases. *J Mol Cell Cardiol*. 2006;41(6):934-948. [CrossRef]
41. Zhang Q, Wang L, Wang S, et al. Signaling pathways and targeted therapy for myocardial infarction. *Signal Transduct Target Ther*. 2022;7(1):78. [CrossRef]
42. Stark K, Massberg S. Interplay between inflammation and thrombosis in cardiovascular pathology. *Nat Rev Cardiol*. 2021;18(9):666-682. [CrossRef]
43. Minhas AMK, Awan MU, Raza M, et al. Clinical and economic burden of percutaneous coronary intervention in hospitalized young adults in the United States, 2004-2018. *Curr Probl Cardiol*. 2022;47(11):101070. [CrossRef]
44. Carberry J, Marquis-Gravel G, O'Meara E, Docherty KF. Where are we with treatment and prevention of heart failure in patients post-myocardial infarction? *JACC Heart Fail*. 2024;12(7):1157-1165. [CrossRef]
45. Caccamo N, La Mendola C, Orlando V, et al. Differentiation, phenotype, and function of interleukin-17-producing human Vgamma9Vdelta2 T cells. *Blood*. 2011;118(1):129-138. [CrossRef]
46. Scapini P, Cassatella MA. Social networking of human neutrophils within the immune system. *Blood*. 2014;124(5):710-719. [CrossRef]
47. Wang C, Zhang C, Wu D, et al. Cholecystokinin octapeptide reduces myocardial fib osis and improves cardiac remodeling in post myocardial infarction rats. *Int J Biochem Cell Biol*. 2020;125:105793. [CrossRef]

48. Hsiao FC, Yeh CN, Chu PH. Regorafenib-related myocardial injury during atrial fibrillation. *Acta Cardiol Sin*. 2016;32(2):243-246. [CrossRef]
49. Wilhelm SM, Dumas J, Adnane L, et al. Regorafenib (BAY 73-4506): a new oral multikinase inhibitor of angiogenic, stromal and oncogenic receptor tyrosine kinases with potent preclinical antitumor activity. *Int J Cancer*. 2011;129(1):245-255. [CrossRef]
50. Dehghani F, Sezavar Seyedi Jandaghi SH, Janani L, Sarebanhassanabadi M, Emamat H, Vafa M. Effects of quercetin supplementation on inflamma ory factors and quality of life in post-myocardial infarction patients: a double blind, placebo-controlled, randomized clinical trial. *Phytother Res*. 2021;35(4):2085-2098. [CrossRef]
51. Dhar K, Moulton AM, Rome E, et al. Targeted myocardial gene expression in failing hearts by RNA sequencing. *J Transl Med*. 2016;14(1):327. [CrossRef]

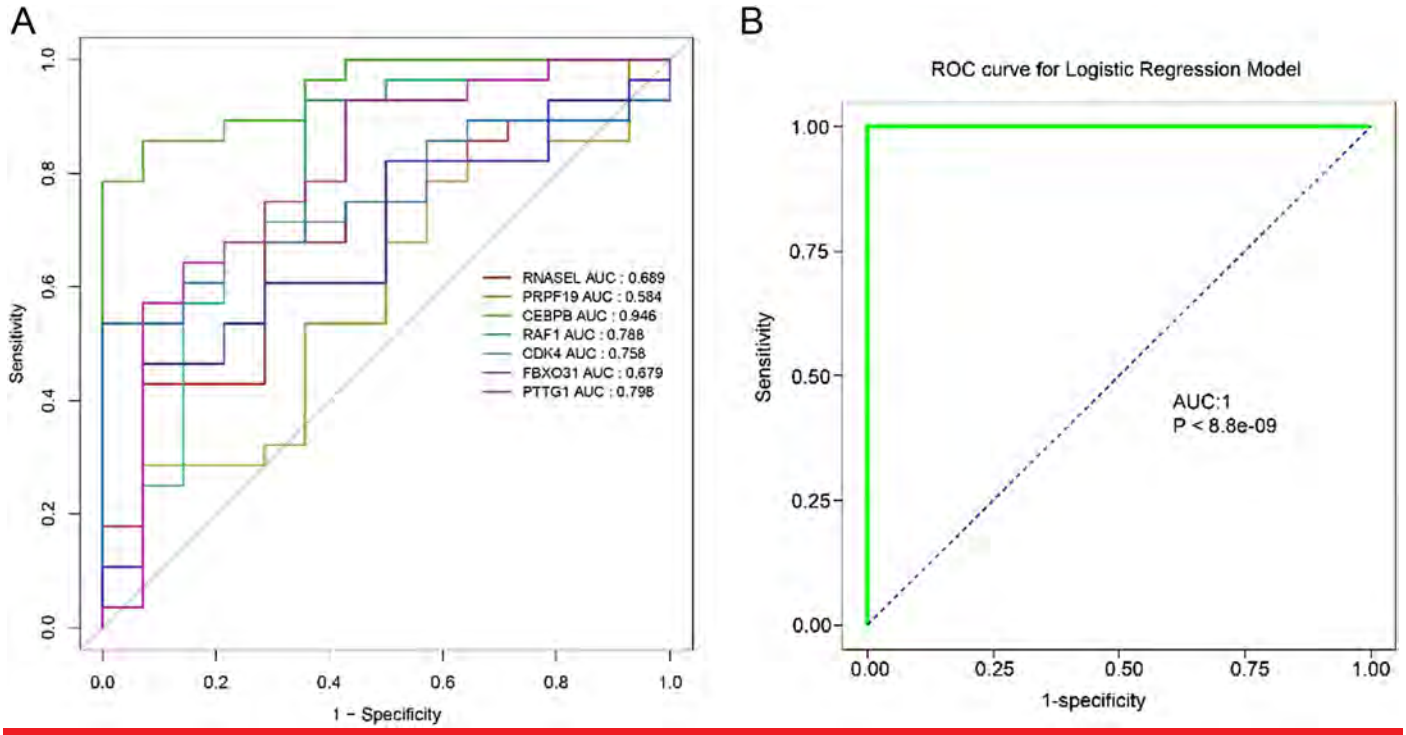

Supplementary Figure 1. The ROC curves of the 7 genes in GSE62646. (A) The single-gene ROC curve of 7 genes; (B) The ROC curve of the 7 genes as a whole in a logistic regression model.